Naked mole rat hyaluronan - an extreme folding biopolymer

Yavuz Kulaberoglu[1], Bharat Bhushan[4], Fazal Hadi[1], Walid T. Khaled[1], Kenneth Rankin[2]*, Ewan[1] St. John Smith[1]*and Daniel Frankel[3]*

[1]Department of Pharmacology, University of Cambridge, Tennis Court Road, Cambridge, CB2 1PD, UK

[2]Northern Institute for Cancer Research, Medical School, Newcastle University, Paul O'Gorman Building, Framlington Place, Newcastle upon Tyne, NE2 4HH, UK

[3]School of Engineering, Newcastle University, Merz Court, Newcastle upon Tyne NE1 7RU, UK.

*Joint corresponding authors: kenneth.rankin@newcastle.ac.uk, es336@çam.ac.uk and daniel.frankel@newcastle.ac.uk

Hyaluronan (HA) is a key component of the extracellular matrix of the cancer-resistant naked mole-rat (NMR). Given the fundamental role of HA in cancer, we undertook to explore the structural and soft matter properties of this ultra-high molecular weight biopolymer. We examined HA extracted from brain, lung, and skin as well as that isolated from the medium of immortalised cells. In common with mouse HA, NMR HA forms a range of assemblies corresponding to a wide distribution of molecular weights. However, unique to the NMR, are highly folded structures, whose characteristic morphology is dependent on the tissue type. Skin HA forms tightly packed assemblies that have spring like mechanical properties in addition to a strong affinity for water. Brain HA forms three dimensional folded structures similar to the macroscopic appearance of the gyri and sulci of the human brain. Lung HA forms an impenetrable mesh of interwoven folds in a morphology that can only be described as resembling a snowman. All of these readily form robust gels without the need for chemical cross-linking and sharply transition from viscoelastic to elastic like properties upon dehydration or repeated loading. Given the role of HA in maintaining hydration in the skin it is plausible that these folded structures contribute to both the elasticity and youthfullness of NMR skin. It is also possible that such densely folded structures could present a considerable barrier to cell invasion throughout the tissues.

Introduction

Hyaluronan (HA), also known as hyaluronic acid, is an extracellular matrix (ECM) polymer found in most tissues.[1,2] Three key enzymes are involved in HA synthesis, HA synthase 1, 2 and 3 (HAS1-3), and it is subsequently broken down by hyaluronidase.[3] The regulation of HA turnover is highly important with there being a clear link between HA metabolism and cancer progression, an abundance of HA being an indicator of poor patient prognosis for a number of tumours.[4–8] HA's role in disease

progression is perhaps unsurprising given its function in cell-ECM interactions.[9–11] The main HA receptor is CD44, a cell surface adhesion receptor that binds a range of ligands and is itself associated with metastasis.[12] The biological function of HA is often related to its molecular weight with a range of polymer sizes found depending on tissue of origin.[13,14] Given the importance of ECM-cell interactions in disease progression and HA-cell interaction in particular, it would be intriguing to examine the structure/assembly of HA in a cancer resistant species.

The naked mole-rat (NMR) has a remarkable biology. They can live for up to ten times longer than similarly sized rodents and rarely develop cancer.[15–17] In 2013 a paper reported that the HA contributed to the animal's cancer resistance.[18] Moreover, the authors reported that it was likely the ultrahigh molecular weight form of HA found in the NMR that contributed to the elasticity of its characteristic wrinkly skin. With such unusual functions attributed to NMR HA it raises the question of if there is anything in its structure or soft matter properties that could explain its functionality.

The majority of data on the structure/assembly behaviour of HA almost exclusively comes from material that is obtained from the fermentation of bacteria (commercially available).[19,20] Less commonly it is sourced from rooster combs or human fluids and tissues. Whether imaged under aqueous conditions or in air, HA is found to form planar branched networks of fibres.[21] Scott et al used rotary shadow electron microscopy to show that HA (extracted from rooster combs, *Streptococci* and mesothelioma fluid) forms planar networks in solution, and that the longer the HA molecule, the more branching occurs.[22] More recent studies have used atomic force microscopy (AFM) in air (as opposed to in aqueous solution) to interrogate the morphology of just a few molecules at the nanoscale. Both loose coils of a few chains and extended structures were observed to assemble with characteristic planar branched network structures common.[19,21,23,24] Using AFM-based force spectroscopy it has been possible to uncoil and unstretch single HA chains and confirm network structures.[25] At the macroscopic scale and in isolation, HA only forms a weak gel and needs to be either chemically crosslinked or combined in a composite to be useful as a biomaterial.[26]

It is well established that HA structural changes over time are fundamental to the ageing of human skin, with its affinity for water thought to be critical for maintaining skin elasticty.[27] To date there has been no attempt to look at the structure or soft matter properties of HA from NMR. Therefore, the aim of this work was to perform the first characterisation of NMR HA via the extraction and purification of HA from a number of NMR tissues and the culture media of NMR immortalised cell lines in order to examine the soft matter properties.

Results

The first tissue examined was skin as the characteristic wrinkly, yet stretchy skin of the NMR has been speculatively attributed to the presence of a high molecular weight HA.[18] Using a biotinylated version of the very specific and tightly binding hyaluronan binding protein (HABP),[28] histological analysis of the plantar surface, forepaw skin demonstrated that HA was present in both mouse and NMR skin. However, HA was observed to a much greater extent in the NMR epidermis compared to the mouse where, as others have shown,[29] HA was largely confined to the dermis (Figure 1A and 1B). HA extracted from the culture medium of immortalised NMR skin fibroblasts

presented a range of assembled conformations, whereby individual chains could clearly be resolved (Figure 1 C and D). Dimensions of these chains were consistently single polymer molecules with an average width of 33.6 ± 7.71 nm (n=100). The most abundant structures within a sample were well defined, densely packed supercoils (Figure 1E). The folds/coils are significantly larger in thickness and height than the individual chains previously mentioned with the structures being up to one micron in height. Scanning electron microscopy confirms the presence of these supercoils, with each structure exhibiting a cauliflower-like presentation (Figure 2A and 2B). Such densely folded entities appear to be the basic unit of HA in NMR skin. In order to confirm this observation, NMR HA was extracted from skin tissue (rather than from the medium of cultured skin fibroblasts) and the same supercoiled folded structures were observed in abundance (Figures 2C and 2D, supplementary Figure 1), although they were generally larger than those of HA extracted from culture medium.

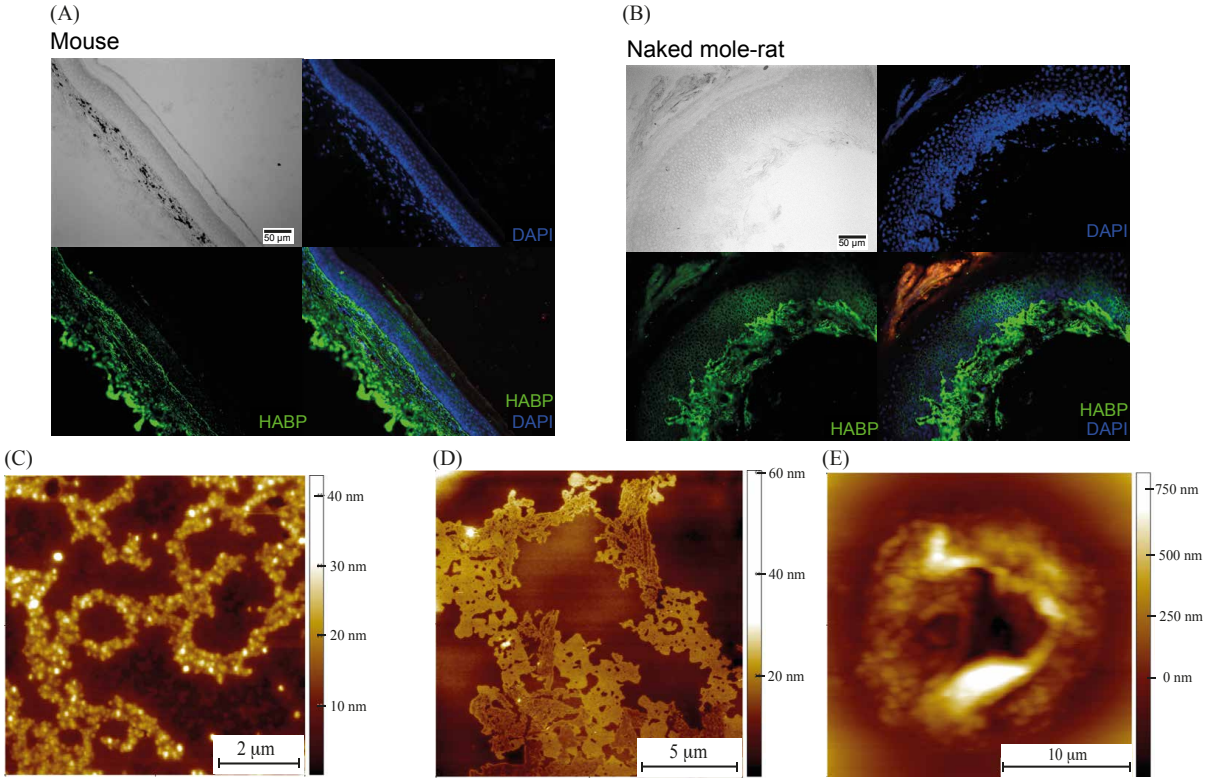

Figure 1 – NMR skin HA. (A) Mouse forepaw, plantar skin section stained for HA using HABP and streptavidin-Alexa488 (green) and DAPI nuclear stain (blue). (B) NMR forepaw, plantar skin section stained for HA using HABP and streptavidin-Alexa488 (green) and DAPI nuclear stain (blue). Unlike in the mouse, the NMR HA extends deep into the epidermis and is significantly more abundant. (C) AFM topography image of HA chains obtained from HA extracted from the media of NMR skin fibroblasts. (D) AFM topography image of another type of HA chain assembly from NMR skin fibroblasts. (E) AFM topography image of supercoiled NRM HA structure. These are highly folded structures up to a micron in height and with some folds/twists half a micron in diameter. All AFM images were taken in contact mode in air.

In the same manner, HA was extracted from NMR brain and lung tissue. HA extracted from whole brain forms large (at least several microns in diameter) supercoils, but this

time the folds were less dense and resembled the macroscopic appearance of the gyri and sulci of the human brain (Figure 3A, B, C). HA extracted from NMR lung also forms supercoils, but this time the characteristic folded structure resembles a morphology which can only be described as resembling a snowman, (Figure 3D and E). Higher resolution images reveal these unusual morphologies to be composed of a network of woven chains, at high density (Figure 3F). Both brain and lung HA structures are very tightly folded with few visible gaps. This is in stark contrast to HA extracted from mouse skin and medium from immortalised mouse skin fibroblasts and human skin, whereby supercoils are not formed and random networks of chains are the dominant structures. (Supplementary Figure 2 and 3) Commercially available HA (high molecular weight produced by microbial fermentation of *Streptococcus pyogenes*, R and D systems) formed branched networks (Supplementary Figure 4). We note that different lentiviral vectors were used to immortalise mouse and NMR skin fibroblasts, the medium from which was used to extract HA, however, the consistency of samples between tissues and cells for both mouse and NMR suggests that the immortalisation method did not make a substantial difference to the results obtained.

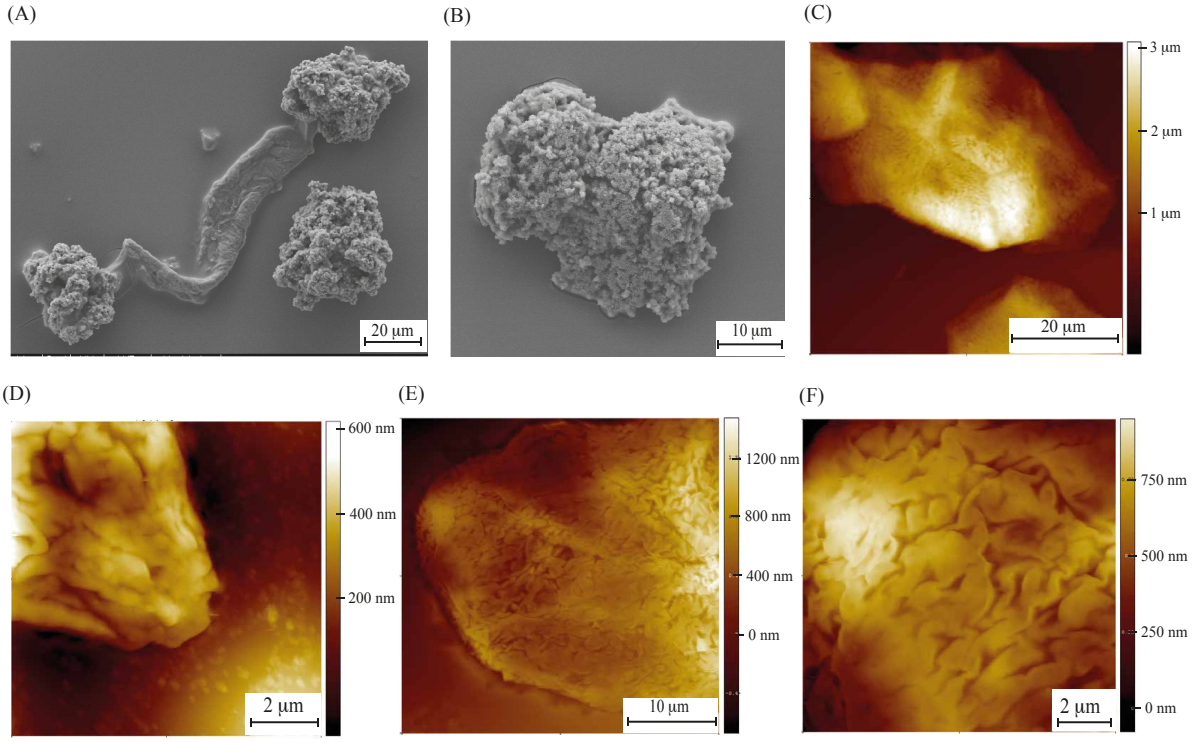

Figure 2 – NMR skin HA. (A) Scanning electron microscopy (SEM) of NMR HA extracted from NMR skin fibroblast media. Supercoils linked together with a large fibre. (B) SEM of NMR HA extracted from NMR skin fibroblast media exhibiting characteristic "cauliflower" appearance. (C) AFM topographic image showing large extremely folded HA coils extracted from NMR skin tissue. (D) AFM topographic image showing large detail of HA folds from NMR skin tissue. (E) Another example of a densely folded HA structure extracted from NMR skin tissue. (F) High resolution image of HA structure (D) exhibiting folding morphology.

Using a conical AFM tip it was possible to address individual supercoils and determine their soft matter properties via indentation. A typical force - separation curve for NMR HA extracted from skin is presented in Figure 4A. Of particular note are the peaks in the red retract curve that represent the unfolding of polymer chains. This is not a

uniform sawtooth pattern, with the irregularity in terms of widths of the peaks, reflective of the different sized folded domains. An unusual feature of this pattern is the peaks in the indentation profile, an interpretation of which would be an unfolding of the structure under compression. More examples of these unusual curves are shown in supplementary material (Supplementary Figure 5). Indentation profiles with peaks in the indentation curve were only seen for the skin supercoils. Upon submerging the supercoils in water (room temperature) a transition occurs in their mechanical properties. After 10 minutes submerged in water the supercoil retains its ability to be unfolded (Figure 4B), but then after 20 minutes the force-separation curve takes the characteristic form of a viscoelastic material (Figure 4C). In order to accurately measure the Young's modulus of supercoils a spherical probe was used. After repeated indentation in the same position the supercoils undergo a transition to a purely elastic material (Figure 4D). This repeated loading (sometimes up to 150 indents at a force of up to 50 nN) appears to squeeze out the water. The transition is sudden with the force distance curve changing form between two consecutive indentations. The purely elastic state can also be reached by dehydrating the HA. Supercoils from all three NMR tissues tested (skin, brain and lung) form microgels when hydrated.

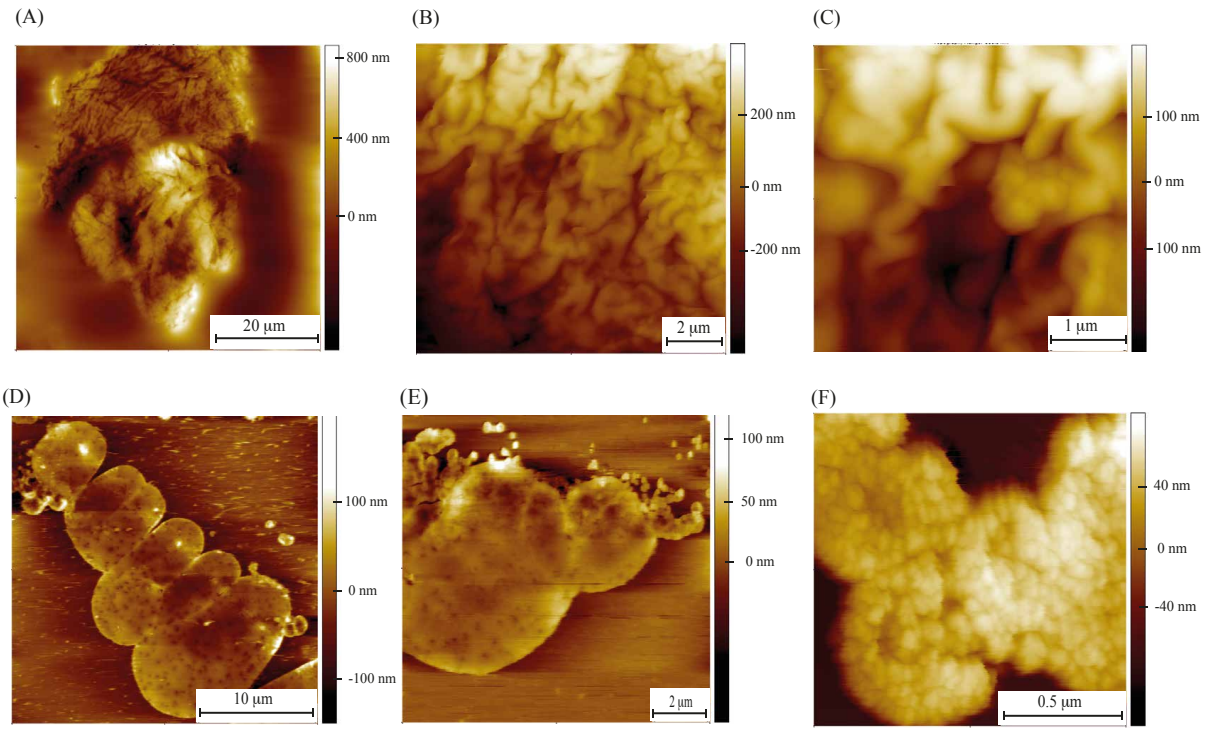

Figure 3 – NMR HA extracted from brain and lung. (A) AFM Topographic image of folded NMR HA extracted from whole brain (B) AFM image showing the folded structure of NMR brain supercoils (C) High resolution topographic AFM image exhibiting characteristic "brain-like" folds of HA extracted from NMR whole brain. (D) HA extracted from NMR lung forms characteristic "snowman" structures. (E) Another example of an NMR lung HA "snowman". (F) Higher resolution scan of HA from NMR lung where the densely folded chains can be resolved, forming an impenetrable network.

Using a spherical probe and fitting the indentation curve to the Hertz model, the Young's modulus of the microgels was determined. These were 10.208 ± 1.677 kPa,

10.435 ± 1.312 kPa, 7.862 ± 0.835 kPa, for NMR skin, brain and lung tissue respectively. A typical modulus distribution taken from close to 1000 indentation curves is shown in Figure 4F. Elastic supercoils (after dehydration) have far superior mechanical properties than the micro gels, for example NMR brain supercoils have a Young's modulus of 30.305 ± 1.541 MPa (n =1499).

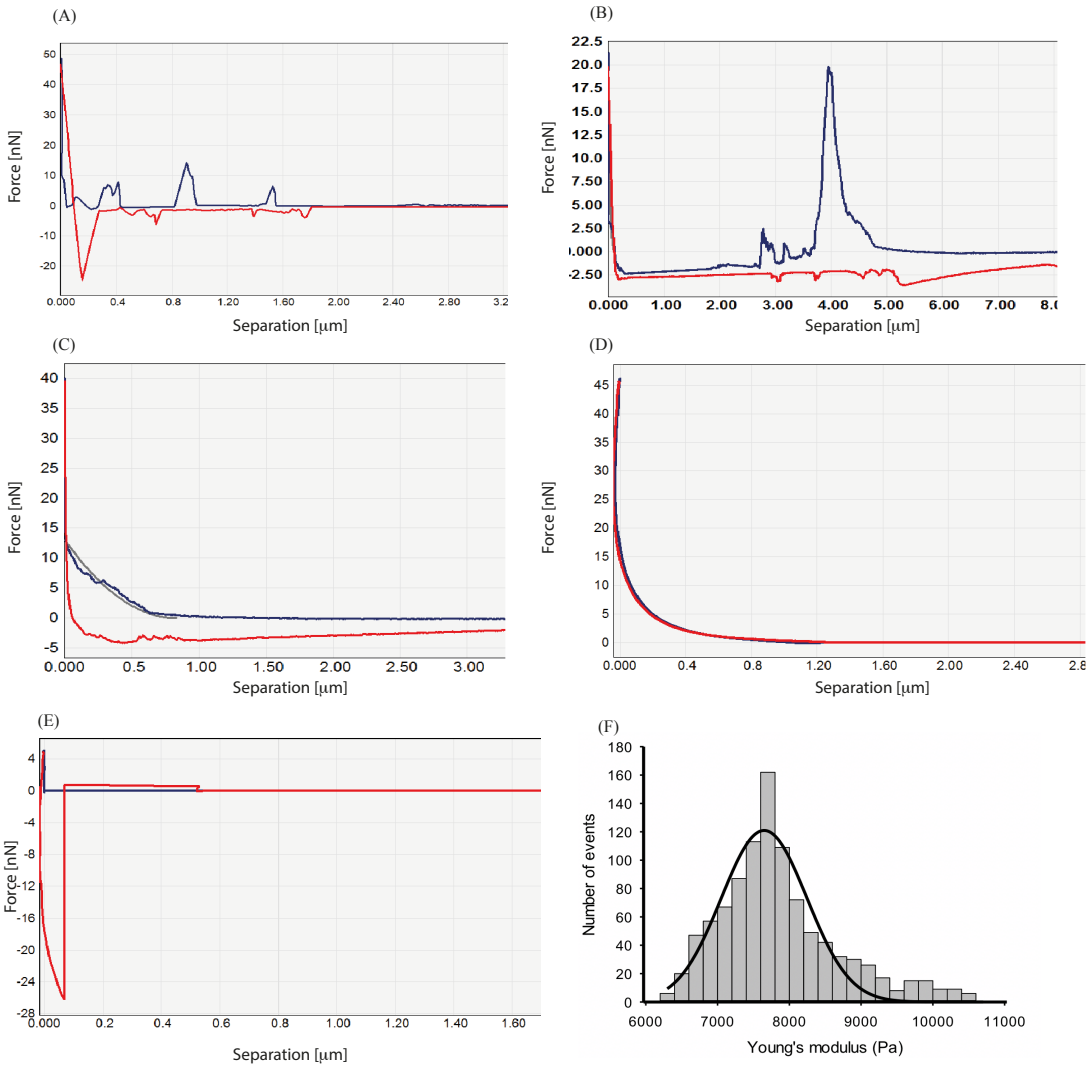

Figure 4 – Mechanical properties of super coiled NMR skin HA. (A) Force-separation curve (pyramidal tip) for an NMR skin HA supercoil measured in air. The retraction curve (red) of the AFM tip exhibits several peaks over a length of microns suggesting the unfolding of large HA chains. Unusually for a force-separation curve, the approach curve (blue) also exhibits a number of force peaks. We attribute these to the force required to push the supercoiled chains out of the way as the tip penetrates through the structure. (B) Force-separation curve for the same supercoil measured in A, but this time being submerged in water. This measurement is after 10 minutes and shows that for this brief amount of time the supercoil retains its ability to be unfolded/folded. (C) The same supercoil indented after 20 minutes submerged in water. The coil now has the characteristic indentation profile of a viscoelastic materials. (D) The indentation curve for lung NMR HA after having been hydrated for an hour. It has the characteristic form for a hydrogel. (E) The indentation curve for the

same supercoil having been indented multiple times (more than 100) in the same place. The water has been squeezed out and the supercoil now has the characteristics of a purely elastic material. (F) Histogram of Young's modulus values (spherical probe) for hydrated HA supercoils derived from lung tissue with a mean value of 7.862 ± 0.835 kPa (n=999 curves taken over 5 coils from tissue from 2 animals).

Although the exact concentration could not be determined for such small amounts of biopolymer, the ability of NMR HA to form gels without the need for chemical crosslinking is interesting. The inability of commercially available HA to spontaneously form robust gels is extensively reported in the literature, with chemical crosslinking or incorporation into a composite being a necessity for practical use as a biomaterial;.[26,30,31]

For HA extracted from all NMR tissues, that is brain, lung and skin, robust macroscopic gels would spontaneously form by leaving 30 ul of HA solution (HA extract in water) on the mica surface for 15 minutes to dry leaving a circular gel up to a cm in diameter, (Figure 5A and 5D). HA extracted from the culture medium of immortalised NMR skin fibroblasts showed the same gelling behaviour, unlike HA from mouse or human skin. As the gel dehydrates the constituent microgels are clearly visible (Figure 5B). The gels have well defined borders (Figure 5C) and the constituent supercoils are recovered upon subsequent dehydration (Figure 5E). A model of how the supercoil swells while retaining its structure is presented in Figure 5F.

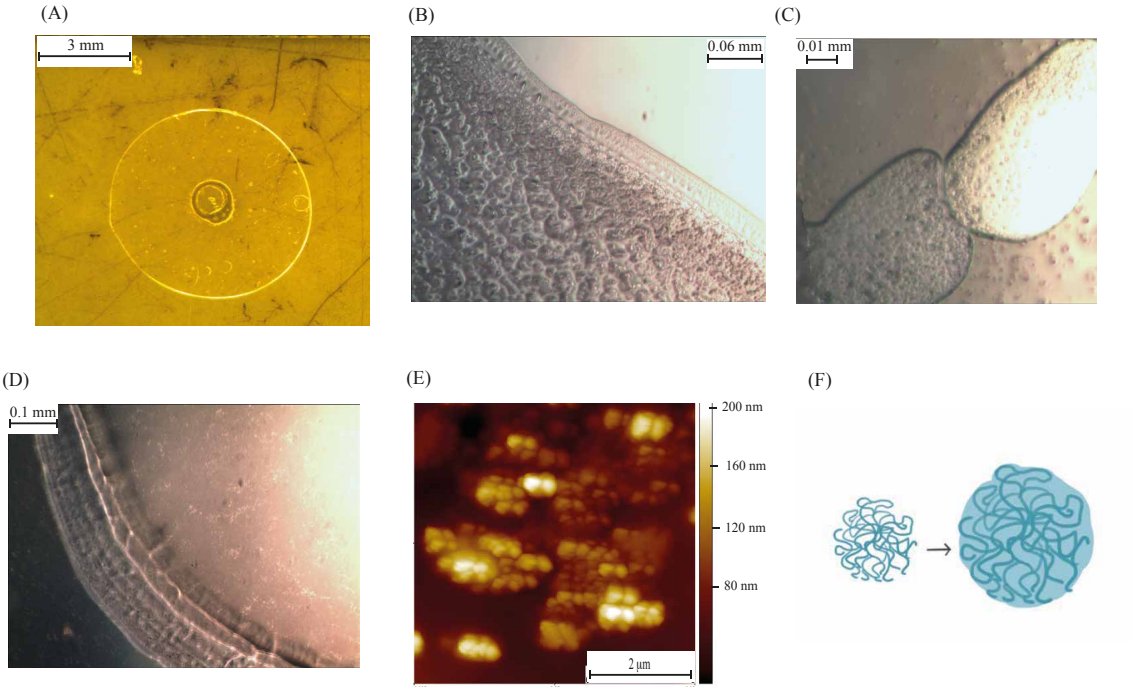

Figure 5 – (A) Macroscopic gel formed from NMR HA extracted from skin tissue. (B) Edge of macroscopic gel formed from brain NMR HA. (C) NMR HA gel particles from (derived from brain tissue) (D) Edge of macroscopic gel formed from NMR lung HA. (E) AFM tapping mode image showing the supercoiled structure is retained after drying, rehydrating for 1 hour, and drying again. (F) Cartoon of an NMR supercoil swelling in water while retaining its overall form. In the dried state (left) the polymer chains have the potential to stretch and unfold, while in the swollen state (right) the chains have less degrees of freedom

Discussion

The nature of NMR HA folding is unusual. It forms a conformation similar to a ball of rubber bands and for the case of HA extracted from skin this leads to a unique indentation profile. A large body of work has been performed on the indentation and unfolding on soft biological matter including proteins, fibres such as collagen, cell membranes, lipid bilayers, and carbohydrates.[32–35] However, it is rare to find a material that has a sawtooth in an indentation curve (as opposed to a retraction curve). One example where this does occur is in amyloid fibrils found in natural adhesives.[36] Such an ability to deform elastically in multiple directions would be advantageous for a material that is subjected to shear forces such as those experienced by the skin whilst an animal is squeezing up and round littermates in tunnels. Given the presence of relatively high quantities of HA in NMR skin (Figure 1B),[18] it is plausible that these supercoils contribute to its elastic nature. These supercoils with their characteristic cauliflower-like structure are absent from HA extracted from human and mouse skin, as well as being absent from commercially available, bacterially produced HA. In terms of HA structure-function relationships it is well established that the molecular weight of HA can relate to function in the tissue of origin[37]. For the case of the NMR the ultrahigh molecular weight contributes via supercoiling to the elastic properties of the skin. In addition, the increased surface area of exposed HA will improve water retaining ability, another essential contributor to the anti-ageing properties of NMR skin. This ability to trap water is evidenced by the formation of microgels with the cross linking usually required for robust gels replaced by self-interactions through entangled polymer. Another important feature of the coiled NMR HA is the density of the polymer network. There are few visible gaps due to the folded packing. This is particularly striking when compared to the morphology of human and mouse HA networks. Mimicking the supercoiled structure of NMR HA in either synthetic or engineered natural polymers would be a strategy to explore in recreating the elasticity and anti-ageing effects in tissue engineered skin as well as biomaterials for preventing cell invasion.

Acknowledgments

This work was supported by a Cancer Research UK Multidisciplinary Project Award (C56829/A22053) to KR, EStJS and DF and a Cancer Research UK Career Establishment Award (C47525/A17348) to WTK FH was supported by a Gates Cambridge Trust scholarship.

(1) Girish, K. S.; Kemparaju, K. The Magic Glue Hyaluronan and Its Eraser Hyaluronidase : A Biological Overview. **2007**, *80*, 1921–1943.
(2) Hargittai, Æ. M.; Szent-gyo, A. Molecular Structure of Hyaluronan : An Introduction. **2008**, 697–717.
(3) Rankin, K. S.; Frankel, D. Hyaluronan in Cancer – from the Naked Mole Rat to Nanoparticle Therapy. *Soft Matter* **2016**, *12* (17), 3841–3848.
(4) Cheng, X. B.; Sato, N.; Kohi, S.; Yamaguchi, K. Prognostic Impact of Hyaluronan and Its Regulators in Pancreatic Ductal Adenocarcinoma. *PLoS One* **2013**, *8* (11), 1–7.
(5) Auvinen, P.; Tammi, R.; Kosma, V.-M.; Sironen, R.; Soini, Y.; Mannermaa, A.; Tumelius, R.; Uljas, E.; Tammi, M. Increased Hyaluronan Content and Stromal

Cell CD44 Associate with *HER2* Positivity and Poor Prognosis in Human Breast Cancer. *Int. J. Cancer* **2013**, *132* (3), 531–539.

(6) Sato, N.; Kohi, S.; Hirata, K.; Goggins, M. Role of Hyaluronan in Pancreatic Cancer Biology and Therapy: Once Again in the Spotlight. *Cancer Sci.* **2016**, *107* (5), 569–575.

(7) Tammi, R. H.; Kultti, A.; Kosma, V.-M.; Pirinen, R.; Auvinen, P.; Tammi, M. I. Hyaluronan in Human Tumors: Pathobiological and Prognostic Messages from Cell-Associated and Stromal Hyaluronan. *Semin. Cancer Biol.* **2008**, *18* (4), 288–295.

(8) Ricciardelli, C.; Russell, D. L.; Ween, M. P.; Mayne, K.; Suwiwat, S.; Byers, S.; Marshall, V. R.; Tilley, W. D.; Horsfall, D. J. Formation of Hyaluronan- and Versican-Rich Pericellular Matrix by Prostate Cancer Cells Promotes Cell Motility. *J. Biol. Chem.* **2007**, *282* (14), 10814–10825.

(9) Qhattal, H. S. S.; Liu, X. Characterization of CD44-Mediated Cancer Cell Uptake and Intracellular Distribution of Hyaluronan-Grafted Liposomes. *Mol. Pharm.* **2011**, *8* (4), 1233–1246.

(10) Clark, R. A.; Alon, R.; Springer, T. A. CD44 and Hyaluronan-Dependent Rolling Interactions of Lymphocytes on Tonsillar Stroma. *J. Cell Biol.* **1996**, *134* (4), 1075–1087.

(11) Richter, U.; Wicklein, D.; Geleff, S.; Schumacher, U. The Interaction between CD44 on Tumour Cells and Hyaluronan under Physiologic Flow Conditions: Implications for Metastasis Formation. *Histochem. Cell Biol.* **2012**, *137* (5), 687–695.

(12) Senbanjo, L. T.; Chellaiah, M. A. CD44: A Multifunctional Cell Surface Adhesion Receptor Is a Regulator of Progression and Metastasis of Cancer Cells. *Front. Cell Dev. Biol.* **2017**, *5* (March).

(13) Cyphert, J. M.; Trempus, C. S.; Garantziotis, S. Size Matters : Molecular Weight Specificity of Hyaluronan Effects in Cell Biology. *Int. J. Cell Biol.* **2015**, *2015*.

(14) Jre, A. F.; Tc, L.; Ubg, L.; Fraser, J. R.; Laurent, T. C.; Laurent, U. B. Hyaluronan: Its Nature, Distribution, Functions and Turnover. *J. Intern. Med.* **1997**, *242* (1), 27–33.

(15) Ruby, J. G.; Smith, M.; Buffenstein, R. Naked Mole-Rat Mortality Rates Defy Gompertzian Laws by Not Increasing with Age. *Elife* **2018**, *7*, 1–18.

(16) Schuhmacher, L.-N.; Husson, Z.; St. John Smith, E. The Naked Mole-Rat as an Animal Model in Biomedical Research: Current Perspectives. *Open Access Anim. Physiol.* **2015**, *7*, 137–148.

(17) Buffenstein, R. Negligible Senescence in the Longest Living Rodent, the Naked Mole-Rat: Insights from a Successfully Aging Species. *J. Comp. Physiol. B Biochem. Syst. Environ. Physiol.* **2008**, *178* (4), 439–445.

(18) Tian, X.; Azpurua, J.; Hine, C.; Vaidya, A.; Myakishev-rempel, M.; Ablaeva, J.; Mao, Z. High-Molecular-Mass Hyaluronan Mediates the Cancer Resistance of the Naked Mole Rat. 1–6.

(19) Cowman, M. K.; Spagnoli, C.; Kudasheva, D.; Li, M.; Dyal, A.; Kanai, S.; Balazs, E. a. Extended, Relaxed, and Condensed Conformations of Hyaluronan Observed by Atomic Force Microscopy. *Biophys. J.* **2005**, *88* (1), 590–602.

(20) Liu, C.; Wang, M.; An, J.; Thormann, E.; Dėdinaitė, A. Hyaluronan and Phospholipids in Boundary Lubrication. *Soft Matter* **2012**, *8* (40), 10241–10244.

(21) Murai, T.; Hokonohara, H.; Takagi, A.; Kawai, T. Atomic Force Microscopy Imaging of Supramolecular Organization of Hyaluronan and Its Receptor CD44. *IEEE Trans. Nanobioscience* **2009**, *8* (4), 294–299.
(22) Scott, J. E.; Cummings, C.; Brass, A.; Chen, Y. Secondary and Tertiary Structures of Hyaluronan in Aqueous Solution, Investigated by Rotary Shadowing-Electron Microscopy and Computer Simulation. Hyaluronan Is a Very Efficient Network-Forming Polymer. *Biochem. J.* **1991**, *274* (Pt 3), 699–705.
(23) Spagnoli, C.; Korniakov, A.; Ulman, A.; Balazs, E. a; Lyubchenko, Y. L.; Cowman, M. K. Hyaluronan Conformations on Surfaces: Effect of Surface Charge and Hydrophobicity. *Carbohydr. Res.* **2005**, *340* (5), 929–941.
(24) Cowman, M. K.; Li, M.; Balazs, E. a. Tapping Mode Atomic Force Microscopy of Hyaluronan: Extended and Intramolecularly Interacting Chains. *Biophys. J.* **1998**, *75* (4), 2030–2037.
(25) Giannotti, M. I.; Rinaudo, M.; Vancso, G. J. Force Spectroscopy of Hyaluronan by Atomic Force Microscopy: From Hydrogen-Bonded Networks toward Single-Chain Behavior. *Biomacromolecules* **2007**, *8* (9), 2648–2652.
(26) Luan, T.; Wu, L.; Zhang, H.; Wang, Y. A Study on the Nature of Intermolecular Links in the Cryotropic Weak Gels of Hyaluronan. *Carbohydr. Polym.* **2012**, *87* (3), 2076–2085.
(27) Papakonstantinou, E.; Roth, M.; Karakiulakis, G. A Key Molecule in Skin Aging Hyaluronic Acid. *Dermatoendocrinol.* **2012**, No. December, 253–258.
(28) Ripellino, J. A.; Klinger, M. M.; Margolis, R. U.; Margolis, R. K. The Hyaluronic Acid Binding Region as a Specific Probe for the Localization of Hyaluronic Acid in Tissue Sections. *J. Histochem. Cytochem.* **1985**, *33*, 1060–1066.
(29) Lee, S. E.; Jun, J. E.; Choi, E. H.; Ahn, S. K.; Lee, S. H. Stimulation of Epidermal Calcium Gradient Loss Increases the Expression of Hyaluronan and CD44 in Mouse Skin. *Clin. Exp. Dermatol.* **2010**, *35* (6), 650–657.
(30) Crescenzi, V.; Francescangeli, A.; Renier, D.; Bellini, D. New Cross-Linked and Sulfated Derivatives of Partially Deacetylated Hyaluronan: Synthesis and Preliminary Characterization. *Biopolymers* **2002**, *64* (2), 86–94.
(31) Yang, Y. L.; Kaufman, L. J. Rheology and Confocal Reflectance Microscopy as Probes of Mechanical Properties and Structure during Collagen and Collagen/Hyaluronan Self-Assembly. *Biophys. J.* **2009**, *96* (4), 1566–1585.
(32) Su, T.; Purohit, P. K. Mechanics of Forced Unfolding of Proteins. *Acta Biomater.* **2009**, *5* (6), 1855–1863.
(33) Lü, J.; Yang, J.; Dong, M.; Sahin, O. Nanomechanical Spectroscopy of Synthetic and Biological Membranes. *Nanoscale* **2014**, *6* (13), 7604–7608.
(34) Baldwin, S. J.; Quigley, A. S.; Clegg, C.; Kreplak, L. Nanomechanical Mapping of Hydrated Rat Tail Tendon Collagen i Fibrils. *Biophys. J.* **2014**, *107* (8), 1794–1801.
(35) Fisher, T. E.; Marszalek, P. E.; Fernandez, J. M. Stretching Single Molecules into Novel Conformations Using the Atomic Force Microscope. *Nat. Struct. Biol.* **2000**, *7* (9), 719–724.
(36) Mostaert, A. S.; Jarvis, S. P. Beneficial Characteristics of Mechanically Functional Amyloid Fibrils Evolutionarily Preserved in Natural Adhesives. *Nanotechnology* **2007**, *18* (4).
(37) Cowman, M. K.; Lee, H.-G.; Schwertfeger, K. L.; McCarthy, J. B.; Turley, E. A. The Content and Size of Hyaluronan in Biological Fluids and Tissues. *Front. Immunol.* **2015**, *6* (June), 261.

(38) Hutter, J. L.; Bechhoefer, J. Calibration of Atomic-Force Microscope Tips. *Rev. Sci. Instrum.* **1993**, *64* (7), 1868–1873.

Materials and methods

Animals

All animal experiments were conducted in accordance with the United Kingdom Animal (Scientific Procedures) Act 1986 Amendment Regulations 2012 under a Project License (70/7705) granted to E. St. J. S. by the Home Office; the University of Cambridge Animal Welfare Ethical Review Body also approved procedures. Young adult NMR (both male and female) were used in this study. Animals were maintained in a custom-made caging system with conventional mouse/rat cages connected by different lengths of tunnel. Bedding and nesting material were provided along with a running wheel. The room was warmed to 28 °C, with a heat cable to provide extra warmth running under 2-3 cages, and red lighting (08:00 – 16:00) was used. NMR were killed by exposure to a rising concentration of CO_2 followed by decapitation. C57Bl6J mice were housed in a temperature controlled (21 ºC) room on a 12-hour light/dark cycle, with access to food and water *ad libitum* in groups of up to five. A female mouse not older than 12 weeks was used for tissue isolation.

Generation of immortalized cells lines

After the animal had been killed, skin was taken from either underarm or underbelly area, cleared of any fat or muscle tissue, generously sprayed with 70% ethanol and finely minced with sterile scalpels. Minced skin was then mixed with 5 ml of NMR Cell Isolation Medium (high glucose DMEM (Gibco #11965092) supplemented with 100 units ml-1 Penicillin, 100µg ml-1 and Streptomycin (Gibco # 15140122) containing 500µl of Cell Dissociation Enzyme Mix (10mg ml^{-1} Collagenase (Roche # 11088793001), 1000Units ml^{-1} Hyaluronidase (Sigma # H3506) in DMEM high glucose (Gibco # 11965092)) and incubated at 37 °C for 3 – 5 hours. Skin was briefly vortexed every 30 minutes to aid cell dissociation and manually inspected for cell dissociation. After complete dissociation, cells were pelleted by centrifuging at 500 g for 5 minutes and resuspended in NMR Cell Culture Medium (DMEM high glucose (Gibco # 11965092) supplemented with 15% fetal bovine serum (Gibco), non-essential amino acids (Gibco # 11140050), 1mM sodium pyruvate (Gibco # 11360039), 100units ml^{-1} Penicillin, 100µg ml^{-1} Streptomycin (Gibco # 15140122) and 100µg ml^{-1} Primocin (InvivoGen # ant-pm-2)), at 32 ˚C, 5% CO_2, 3% O_2. To immortalize NMR skin fibroblasts, a lentiviral plasmid carrying SV40LT (SV40LT-hRASg12v was used for mouse cells) was packaged using HEK293FTs as packaging cells. The supernatant of HEK293FT packaging cells was collected, containing SV40 LT-packaged viral particles. When primary NMR skin cells reached 40% confluency, the supernatant containing SV40-packaged viral particles was added on to the primary NMR skin cells. 48 hours after adding the supernatant, cells were treated with 2 µg/ml of puromycin to kill off uninfected cells. Stable immortalized cells were maintained in DMEM supplemented with 15% fetal bovine serum, non-essential amino acids, sodium pyruvate, 100 units ml^{-1} penicillin, and 100 mg ml^{-1} streptomycin.

HA extraction from NMR tissues:

Following decapitation, tissues were removed, weighed and stored at -80 ºC until HA extraction was conducted. Tissues were digested at 50 ºC overnight in the digestion buffer (10-mM Tris-CL, 25 mM EDTA, 100 mM NaCl, O.5% SDS and 0.1 mg/ml of

Proteinase K). The next day, samples were centrifuged at 18,000 x g for 10 minutes to remove tissue residual particles and supernatant were transferred to a new tube. Four volumes of ethanol were added into the supernatant, followed by incubation overnight at -20 ^{o}C. The following day, samples were cold-centrifuged at 18,000 x g for 10 minutes. Pellets were then washed in four volumes of 75% ethanol by centrifugation. The supernatant was discarded and pellets were incubated at room temperature for 20 minutes to remove any residual ethanol. The pellets were then resuspended in 200 µl of autoclaved distilled water. 500 units of benzonase endonuclease was added and then incubated overnight at 37 ^{o}C to remove nucleic acids. The next day, samples were precipitated overnight with one volume of 100% ethanol. The following day, after cold centrifugation at 18,000 x g for 10 minutes, pellets were resuspended in 400 µl of autoclaved distilled water.

HA extraction from conditioned medium

Immortalized skin fibroblasts were seeded and maintained for 7 days without changing medium. After 7 days, the media from each flask was collected and centrifuged at 4,000 x g for 10 minutes to remove residual cells. After centrifugation, 2 ml of conditioned media were incubated overnight with 500 µg of proteinase K at 50 ^{o}C to remove proteins. The following day, 2 volumes of 100% ethanol were added to samples for precipitation and incubated overnight at -20 ^{o}C. The next day, samples were cold-centrifuged at 18,000 x g for 10 minutes. After centrifugation, supernatant were discarded and pellets were incubated at room temperature for 20 minutes to allow any residual ethanol to evaporate. After the incubation, the pellet was resuspended in 400 µl of autoclaved distilled water.

HA extraction from human skin

Following consent to the Newcastle Academic Health Partner's Bioresource at Newcastle University, skin samples were obtained from patients undergoing orthopaedic surgery. Ethics approval was gained from the REC North East Newcasstle 1, Reference Number: REC 12/NE/0395. Human skin was chopped and weighed amount of skin tissues were digested overnight at 50 ^{o}C in the digestion buffer (10 mM Tris-Cl, 25 mM EDTA, 100 mM NaCl, 0.5 % SDS and 0.1 mg ml^{-1} proteinase K). After centrifugation, a clear supernatant obtained was mixed with four volumes of prechilled ethanol and incubated at -20 ^{o}C for overnight. The precipitate was centrifuged, washed with ethanol and air dried. The pellet was resuspended in 100 mM ammonium acetate solution and incubated with benzonase endonuclease at 37 ^{o}C for overnight to remove nucleic acid. The solution was mixed with four volumes of ethanol and incubated at -20 ^{o}C for overnight. The pellet obtained after centrifugation was again washed, air dried and resuspended in 100 mM ammonium acetate for further use.

HA adsorption onto mica

30 ul of purified NMRHA in water was deposited on freshly cleaved muscovite mica and allowed to dry in air for 45 minutes. This is the method reported by Cowman et al for the AFM imaging of HA[19]. They noted that HA adsorbs weakly to mica and cannot be examined under liquid conditions due to HA's affinity to be in solution. For examining hydrated HA the sample was allowed to dry for 15 minutes so that visible water had evaporated but the sample was still wet.

Scanning Electron Microscopy

Prior to imaging the air-dried HA samples were sputter coated in gold to prevent charging. Imaging was performed on either an XL30 ESEM-FEG or a Jeol JSM-5600LV using the secondary electron detector on each instrument.

Atomic Force Microscopy

All images were obtained on an Agilent 5500 microscope equipped with close loop scanners. Contact mode imaging was employed for topographic imaging using silicon tips having a nominal force constant of between 0.02-0.77 N/m. Forces were minimized during scanning at a level below 1 nN. Scan rates were between 0.5–1 kHz and all images were recorded at 512 pixel resolution. Measurements were carried out in ultrapure water room at room temperature (~20 °C). Processing and analysis of images was performed using version 6.3.3 of SPIP software (Image Metrology, Lyngby, Denmark).

Atomic Force Microscopy Based Nanoindentation

Two different types of tip indentation geometry were used. The first were conical tips with radius of curvature less than 15 nm. These were used to look at unfolding events within a supercoil. Accurate determination of the spring constant was obtained using the using the equipartition theorem as proposed by Hutter and Bechhoefer.[38] Inaccuracies in terms of knowing the contact area between tip and sample in the Sneddon model for conical tips can be compensated for by using a large spherical probe therefore spherical probes were used to determine Young's modulus values. Borosilicate spherical probes 5 μm in diameter (NovaScan Technologies) were used to indent supercoils, both wet and dry. Spring constants were determined using the thermal K method. Indentation curves were fitted with the Hertz model for spheres on a flat surface which assumes that the indent depth is much smaller than the diameter of the probe.

$$F_{Herz} = \frac{4}{3}\frac{E_{surface}}{\left(1-v_{surface}^2\right)}\sqrt{R_{tip}}(s_0 - s)^{3/2}$$

where

F_{Herz} = force

$E_{surface}$ = Young's modulus of the surface

$v_{surface}$ = Surface Poisson's ratio

R_{tip} = ball radius

s_0 = point of zero indentation

s_0-s = indentation depth

Indentation curves were taken across at least 5 supercoils. When tissue extracted samples were used, these originated from three animals. When HA extracted from the medium of immortalised cells were used they curves were taken across three different cell preparations. Only curves that were able to be fitted to the model were used.